university of groningen / faculty of science and engineering

Bachelor Research Project Applied Physics

Environmentally Friendly 2D Tin Lead Perovskite Memristor Fabricated with Blade Coating

S.M.R. Rakibuzzaman

First Examiner: Prof. dr. M.A. Loi
Daily Supervisor: Lijun Chen
Second Examiner: Prof. dr. L.J.A. Koster

July 10, 2023

Abstract

This study explores the fabrication and characterization of environmentally friendly 2D tin lead perovskite memristors using the scalable technique of blade coating. Memristors, a new type of electrical component, only theoretical until recently, offer non-volatility and resistive switching properties, making them suitable for memory applications. Perovskite materials, such as tin lead perovskites, exhibit desirable characteristics like high ON/OFF current ratios and low power consumption, making them ideal for memristor fabrication. The prepared memristors have a smooth surface with a root-mean-square roughness of 0.4 nm, ensuring reproducibility and scalability. Spectral analysis reveals high absorbance in the mid-visible to UV wavelengths, indicating a bandgap energy of approximately 2.068 eV. The memristors demonstrate reliable performance, with good hysteresis within voltage-current graphs stable for up to 38 days, and maximum current On/Off ratios reaching up to 348. These findings highlight the potential of 2D tin lead perovskite memristors in neuromorphic computing, memory applications, and advanced electronics. Further research options include comparative analyses of different materials, fine-tuning fabrication techniques, and exploring lead-free alternatives.

Contents

1 Introduction

The field of applied physics has witnessed remarkable advancements in recent years, paving the way for innovative technologies that are transforming various aspects of our lives. However, with the rapid development of society and the acceleration in data growth, traditional computing architecture encounters the von Neumann bottleneck, which has become an ever-larger obstacle in the process of improving the performance of computing systems. Therefore, emerging non-volatile memory devices have attracted great attention in recent years.

Memristor, the concept was first proposed by Leon Chua in 1971 but was only theoretical [1]. It means that there should be a relationship between the charge and the magnetic flux, the resistance value can be changed by controlling the change of the current, and the memory will not disappear even if the current is interrupted. However, there was no material that could describe this relationship at that time. It was not until the discovery of practical memristors in 2008 [2] that the field gained more attention. Memristors possess the unique ability to remember and store information in a non-volatile way, revolutionizing conventional memory technologies and opening up new possibilities for neuromorphic computation.

Neuromorphic computation, inspired by the structure and functionality of the human brain, is a captivating area of research within applied physics. By emulating the brain's neural networks, neuromorphic systems aim to perform cognitive tasks with much higher efficiency. Memristors play a pivotal role in these systems [3], as their ability to store and process information resembles the behaviour seen in biological systems. As a result, memristor-based architectures hold the potential to unleash powerful and energy-efficient computing paradigms, paving the way for applications such as real-time pattern recognition, machine learning and energy cost reduction [4].

In recent years, different active materials have been used in the memory devices (top-electrode/active layer/bottom-electrode). Inspired by the defect-induced hysteresis observed in current–voltage characteristics of perovskites solar cells, perovskite-based memory devices have aroused great interest owing to the easy deposition process and intrinsic multi-trap state characteristics. Therefore, perovskite memristors have shown desirable characteristics such as high ON/OFF current ratios [5], low power consumption, and multi-level storage capacity, making them a promising choice for efficient and versatile memory elements in neuromorphic computing systems.

The motivation behind exploring 2D tin lead perovskite memristors lies in their unique properties and potential to overcome the limitations associated with lead perovskites, which pose environmental and health hazards due to their toxic nature [6]. Tin lead perovskite, a more sustainable alternative, offers an option for developing high-efficiency and stable computing devices without the downside of environmental toxicity. However, the stability of tin composition presents a challenge due to its susceptibility to degradation in the presence of oxygen and humidity. Therefore, novel 2D perovskites have been proposed for improving environmental instability and repeatability. The insertion of large organic spacer cations leads to both quantum and dielectric confinement of carriers in the octahedral planes.

In addition, most perovskites are deposited using lab-scale spin-coating, which is a wasteful technique that is not possible to prepare in batches on a large scale. Blade coating is a facile method that has a very high precursor utilization rate and allows tuning the deposition temperature. Therefore, in this bachelor's thesis, the main objective of this research project is to investigate the electrical performance of 2D tin-lead perovskite memristors fabricated by blade coating.

In this study, we measured the IV curves in a nitrogen-filled chamber without oxygen and humidity. The aim is to gain insights into the behaviour and performance of 2D tin lead perovskite memristors. In addition, their electrical performance degradation over time through IV curve measurements was

performed. Moreover, the potentiation and depression properties of the memristors are studied for their neuromorphic applications. Taking sustainability and environmental safety as a focus point, this study aims to overcome the challenges associated with lead perovskites and explore the potential applications of tin lead perovskite memristors in next-generation computing architecture.

2 Theoretical Background

Memristors have emerged as promising electronic devices revolutionizing computing architecture. In this context, the field of perovskite memristors has gained attention due to its potential for efficient and versatile memory elements. However, stability issues related to oxygen and humidity sensitivity pose significant challenges. This study focuses on 2D tin lead perovskite memristors, which offer unique properties and potential solutions for overcoming these limitations. Theoretical foundations encompass memristor fundamentals, perovskite materials, IV curve analysis, and their relevance to neuromorphic and Von Neumann computer architectures.

2.1 Memristors: Fundamentals and Characteristics

Most people are aware of the three common circuit elements: the resistor, the capacitor, and the inductor. These elements are defined by their relationship between four key variables: electric current, voltage, charge, and magnetic flux. They can be thought of as interconnected quantities. Resistance (R) represents how voltage changes with current, capacitance (C) represents how charge changes with voltage, and inductance (L) represents how magnetic flux changes with the current. But there was a missing piece in our understanding. The relationship between charge and magnetic flux was undefined. To address this gap, Chua in 1971 [1], proposed the memristor, a hypothetical component with a unique property: its magnitude (M) captures the change in magnetic flux with respect to charge. If the memristor were real, it would have the same unit of measurement as resistance (ohm, Ω). This is illustrated in Figure 1.

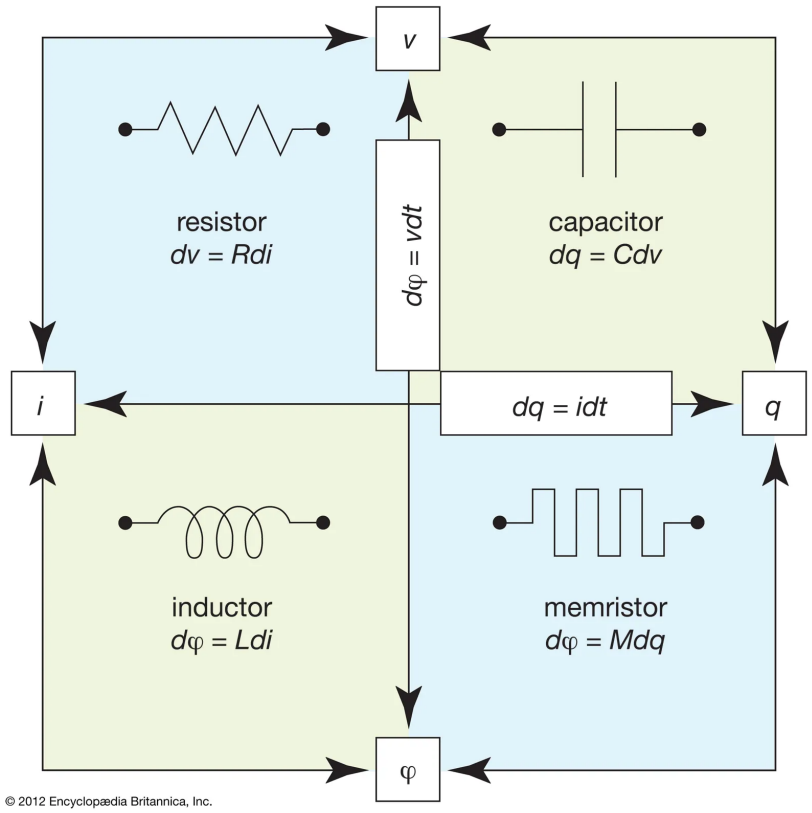

Figure 1: The four fundamental two-terminal circuit elements: resistor, capacitor, inductor, and memristor. Adapted from [7].

This memristor completes the quartet of fundamental circuit elements, accounting for the relationship between charge and magnetic flux. It was a groundbreaking idea that expanded our understanding of circuits and opened up new possibilities for electronic devices.

Memristors possess fundamental properties and characteristics that distinguish them from other circuit elements. One key property is their non-volatility [8], meaning they can retain information even when power is turned off. This characteristic makes memristors suitable for data storage applications, as they can retain their state without the need for a continuous power supply. Another important feature is resistive switching [2], which refers to the ability of memristors to change their resistance in response to an applied voltage. This allows memristors to transition between high and low resistance states, corresponding to the storage of binary information ("0" and "1"). This resistive switching behaviour is at the core of memristor-based memory devices, enabling efficient data storage. In addition, they can remember the resistance state that was previously set and maintain it until a different voltage is applied to switch it to a different state. This memory property is essential for the operation of memristor-based circuits, and it can allow for the storage and retrieval of information. [9].

By combining non-volatility, resistive switching, and memory behaviour, memristors can offer advantages for various applications. They hold promise for the development of high-density, low-power, and high-speed memory technologies [10]. Additionally, their ability to store and process information at the same time resembles the behaviour of biological synapses, making them promising candidates for neuromorphic computing and artificial intelligence applications [11]. Understanding these fundamental properties and characteristics is crucial for unlocking the potential of memristors in advancing future computing and memory systems.

2.2 Perovskites

Perovskite materials have received substantial attention in the field of memristor research. These materials offer some advantages for memristor functionality, such as high ON/OFF current ratios, low power consumption, and multi-level storage capacity [5]. The emergence of perovskite memristors has sparked interest in exploring their advantages over other materials used in memristor technology. Compared to traditional materials, perovskite memristors show higher performance in terms of switching speed, endurance, and scalability [12]. Their favourable electrical properties make them highly promising for efficient and versatile memory elements in neuromorphic computing systems.

Perovskites are a crystal lattice defined with a general ABX_3 chemical structure [13]. Here A and B are cations of different sizes and X is an anion. The A and B cations can be a variety of elements, including metals, while the X anion is typically oxygen or a halogen. This is shown in Figure 2. This flexibility in composition allows for a wide range of perovskite materials with diverse properties.

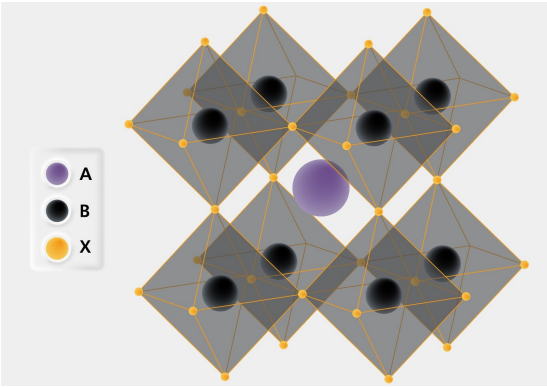

Figure 2: Basic Perovskite ABX_3 molecular structure. Adapted from [14].

Perovskite structures can differ from Figure 2 in key ways such as reduced dimensionality. 2D perovskites are a fascinating class of materials that exhibit unique properties due to their layered structure. Unlike traditional 3D perovskites, which have a three-dimensional crystal lattice, 2D

perovskites consist of stacked layers held together. One advantage of 2D perovskites is their enhanced stability compared to their 3D counterparts [15]. Furthermore, the quantum confinement effect in 2D perovskites leads to interesting optical and electronic properties. These materials exhibit strong photoluminescence and have shown potential for applications in light-emitting diodes (LEDs) and other optoelectronic devices. Figure 3 shows the structure of a 2D perovskite.

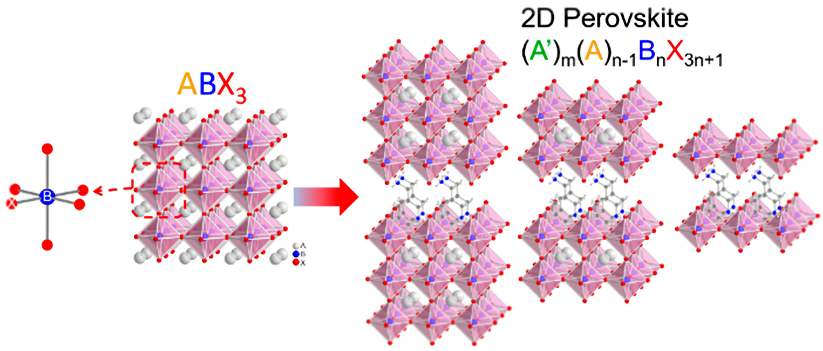

Figure 3: Structural and chemical difference between a 3D and 2D perovskite. Adapted from [16].

There is also a class of perovskites known as organic-inorganic hybrid perovskites where the A cation is an organic cation, the B is an inorganic one and the X is a bridging ligand connecting them A and B together [17]. Hybrid organic-inorganic perovskites are special compared to all inorganic perovskites because they have a rich reservoir of exotic switching physics. This makes them an attractive, inexpensive alternative to designing efficient memristive hardware. They possess very large degrees of freedom or state variables [18].

2.3 Tin Lead Perovskite Memristors

Perovskite materials have garnered significant attention in the field of memristor research, offering a wide range of possibilities for high-performance and sustainable computing systems. While Lead Perovskites have demonstrated desirable properties, such as high carrier mobilities and long charge carrier lifetimes [19], they pose challenges due to their environmental and health hazards caused by the presence of toxic lead [20]. As a result, researchers have turned their focus towards Tin Perovskites as a more environmentally friendly alternative. Tin Perovskites exhibit lower toxicity, and enhanced optoelectronic properties compared to lead perovskites. However, tin perovskites face their limitations, primarily in achieving stability in oxygen and humid environments [21].

To overcome the stability-performance trade-off, a promising solution lies in the exploration of tin-Lead perovskites. By combining tin and lead within the perovskite structure, researchers aim to achieve a favourable middle ground that preserves both stability and performance. Tin-lead perovskites have promising optoelectronic properties like increases in attainable charge-carrier mobilities, decreases in exciton binding energies, and potentially a slowing of charge-carrier cooling, which is relevant for photovoltaic devices [22]. By delving into the structural aspects, fabrication methods, and electrical performance of these materials, researchers seek to uncover their suitability as memristive devices. Additionally, understanding the charge transfer dynamics and the interplay between tin and lead within the perovskite lattice can provide insights into optimizing the stability-performance trade-off.

2.4 IV Curves and Hysteresis

IV (Current-Voltage) curves play a crucial role in characterizing the behaviour of memristors and provide valuable insights into their electrical performance. By plotting the current flowing through a memristor against the applied voltage, IV curves offer a comprehensive understanding of the device's

resistive switching characteristics and its response to external stimuli [23]. Understanding the significance of IV curves and hysteresis phenomena is fundamental to unravel the underlying mechanisms of memristive behaviour.

Hysteresis, a key feature observed in memristors, refers to the dependence of the current-voltage response on the previous electrical history of the device. It manifests as a loop-like pattern in the IV curve, indicating different resistance states depending on the direction of the voltage sweep. The equation for a theoretical pinched loop hysteresis is given by [24],

$$v(t) = A\left[1 + \frac{A^2}{\omega^2}(1 - \cos\omega t)^2\right]\sin\omega t \tag{1}$$

where A and ω are the peak voltage and frequency of a sinusoidal current respectively, and $v(t)$ is the voltage value as it evolves over time. A graphical representation for this is shown in Figure 4.

The presence of hysteresis is directly linked to the resistive switching phenomenon, where the memristor exhibits a reversible change in resistance under the influence of an applied voltage. The hysteresis loop captures the transition between high and low resistance states (HRS and LRS), providing information about the stability, endurance, and reliability of the device.

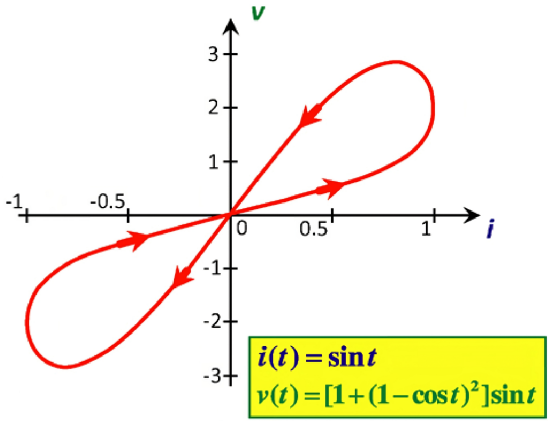

Figure 4: A pinched hysteresis loop is a Lissajous figure with two values for ($v(t)$, $i(t)$). The values of A and ω are both set to 1 here within equation 1. Retrieved from [24].

In the context of perovskite memristors, several research studies have focused on investigating IV curves to understand the electrical behaviour and performance of these materials. Experimental techniques, such as voltage sweep measurements, have been employed to capture the IV characteristics and study the resistive switching mechanisms [18]. By analyzing the IV curves, researchers have gained insights into the factors influencing the switching behaviour, such as the composition of perovskite materials, interfacial effects, and defect states as it does with perovskite solar cells [25].

2.5 Neuromorphic application

In the realm of computer architecture, a significant shift is taking place, with the emergence of neuromorphic computing challenging the traditional Von Neumann architecture. While the Von Neumann architecture has been the foundation of modern computing for decades [26], neuromorphic computing takes inspiration from the human brain's structure and functionality, offering a paradigm shift in computational efficiency and cognitive capabilities [27].

The Von Neumann architecture, named after the renowned mathematician and computer scientist John von Neumann, is based on the separation of memory and processing units. In this architecture, data is stored in a separate memory module and sequentially processed by a central processing unit

(CPU) [28]. While this architecture has been highly successful and versatile, it faces limitations in terms of speed, energy efficiency, and scalability, particularly for tasks that require massive parallelism and cognitive abilities [29].

Neuromorphic computing, on the other hand, is inspired by the intricate neural networks of the human brain. It aims to replicate the brain's efficient and parallel information processing, enabling cognitive tasks with remarkable efficiency [30]. By employing networks of artificial neurons and synapses, neuromorphic systems can perform complex computations in parallel, mimicking the brain's ability to process and recognize patterns, learn, and adapt quickly.

Memristors, with their unique ability to store and process information, play a pivotal role in enabling neuromorphic computation by closely resembling the behaviour of synapses in biological neural networks [31]. These devices exhibit resistance changes based on applied electrical stimuli, retaining information even when power is turned off, akin to synaptic plasticity in the brain. This memristive behaviour facilitates the creation of artificial neural networks with high flexibility, learning capabilities, and adaptability. Integrating memristors into neuromorphic systems offers tremendous potential for future computing architectures, as they provide unprecedented energy efficiency compared to traditional approaches. Memristor-based neuromorphic systems not only significantly reduce power consumption but also enable parallel processing, allowing for real-time data analysis, autonomous decision-making, and intelligent edge computing. This integration holds promise for revolutionizing various domains, including artificial intelligence, robotics, and big data analysis, ushering in a new era of cognitive computing.

3 Method

This section describes the experimental methods for fabricating and characterizing 2D tin lead perovskite-based devices. It is divided into three subsections: 'Device Fabrication', 'Material Physical Properties', and 'Probe Station Measurements'. The 'Device Fabrication' subsection covers substrate preparation, production of the perovskite, coating techniques and electrode deposition. The 'Material Physical Properties' subsection discusses the characterization techniques, including Atomic Force Microscopy (AFM) and Absorbance Measurements. The 'Probe Station Measurements' subsection explains the setup and procedures for conducting current-voltage (IV) and neuromorphic measurements.

3.1 Device Fabrication

The memristor device is composed of several layers stacked on top of each other to maximise the effectiveness of the active layer. The layers are shown in Figure 5 below.

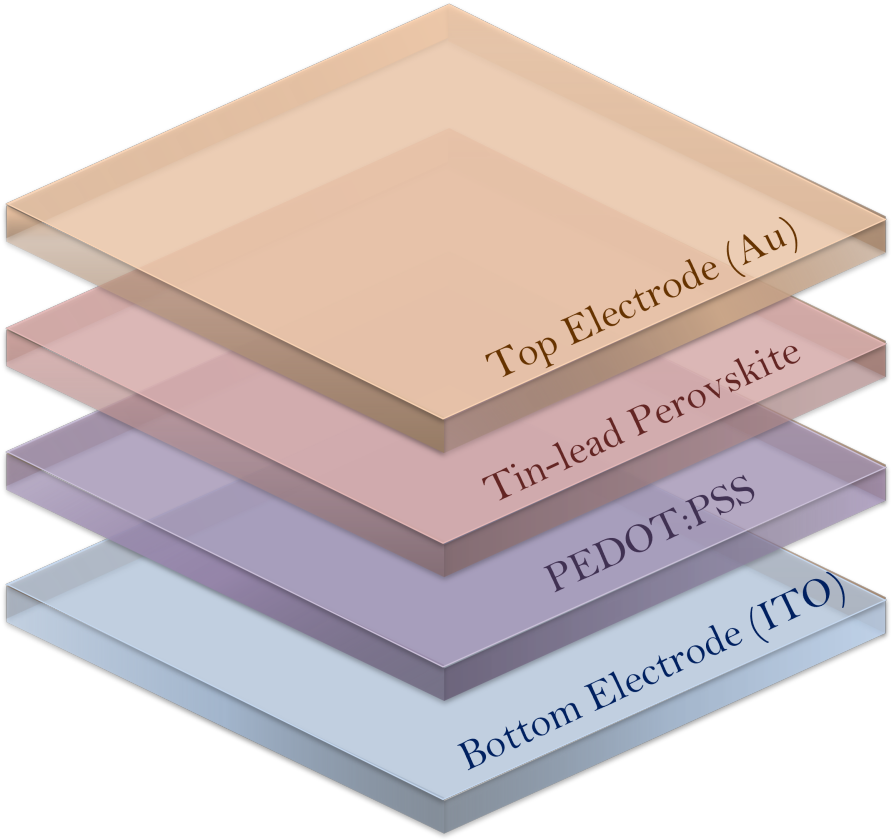

Figure 5: The memristor device structure. [From top to down] The top electrode, is composed of deposited gold, the Tin-Lead Perovskite layer, a PEDOT:PSS conductive polymer layer and the Bottom electrode (Indium Tin Oxide) which is fixed on a glass substrate.

3.1.1 Preparing the Substrate

The samples were prepared in two batches, 8 on the first and 9 on the second batch. The substrate which would serve as the bottom electrode of the memristor device is composed of glass with a layer of Indium Tin Oxide (ITO) predeposited on it in rectangular shapes. This substrate is cleaned in the clean room initially with soap and then set in an ultrasonic bath to get rid of the aforementioned soap. The samples are then soaked in acetone for 15 minutes and isopropyl alcohol for 15 minutes and placed in the ultrasonic bath after each round of soaking.

The samples are put through a UV chamber and an oven at 140°C for 20 minutes each. The samples are blasted with UV light to increase the wettability for the PEDOT:PSS layer. They are put through the oven to anneal the ITO layer to increase its conductivity [32].

3.1.2 Preparing the Perovskite Solution

Due to the high reactivity with oxygen and H_2O, the following procedure is conducted within a glove box. The chemicals needed to formulate, the Tin Lead perovskite are:

$$\text{1,5-DAN} + PbI_2 + SnI_2 + SnF_2 + \text{Solvent (DMF)} \implies DAN_2Pb_{0.5}Sn_{0.5}I_4,$$

where 1,5-DAN is 1,5 Diaminonapthalene which is illustrated in figure 6. The solvent Dimethylformamide (DMF) is used for dissolving the perovskite. The amounts of each of the reagents are 1,5-DAN (0.1 mmol), PbI_2 (0.05 mmol), SnI_2 (0.05 mmol), SnF_2 (0.005 mmol) and DMF (0.5 ml). Due to the low mass of the chemicals, they need to be discharged with an anti-static gun to ensure they do not exit their containers due to repulsion. The solutions were stirred overnight before use, and then filtered with a 0.2μm filter.

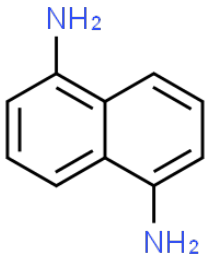

Figure 6: The 2D chemical structure of 1,5 Diaminonapthalene which is a naphthalene-diamine compound having amino substituents in the 1- and 5-positions. Adapted from [33].

3.1.3 Spin and Blade Coating

Poly(3,4-ethylenedioxythiophene)-poly(styrenesulfonate) (PEDOT:PSS), which is a high-conductive polymer used in many areas of solid-state physics research. This organic semiconductor is suitable for electromagnetic shielding and noise suppression due to its high electrical conductivity and good oxidation resistance [34]. It is also transparent to light in a wide part of the EM spectrum. This spin-coated onto the substrate after putting it through a water filter. The spin-coater is spun at 3000 RPM for 30 seconds to evenly coat the substrate with a thickness of 40 μm.

The PEDOT:PSS coated substrates now need to be coated with the prepared perovskite solution. This was achieved using a blade coater which is set at 100 °C. The perovskite solution is deposited onto the edge of the sample using a pipette holding 20 μl. The speed of the blade is set to 80 mm/s to ensure a thickness of 100 μm. The samples are then annealed at 100 °C for 10 minutes. Blade coating is relevant for the scalability and sustainability of the production of 2D perovskites as it can easily be scaled for industrial applications and reduce wastage when compared to traditional coating methods like spin coating [35]. This method is illustrated in Figure 7.

3.2 Vapour Deposition of the Top Electrode

Vacuum Deposition is a thin film deposition technique performed under vacuum conditions. In this process, gold metal is vaporized using an electron beam or resistance heating source within a vacuum chamber. The vaporized gold atoms then condense onto the surface of the perovskite layer, forming a uniform and adherent gold film. This process allows for precise control over the thickness of the

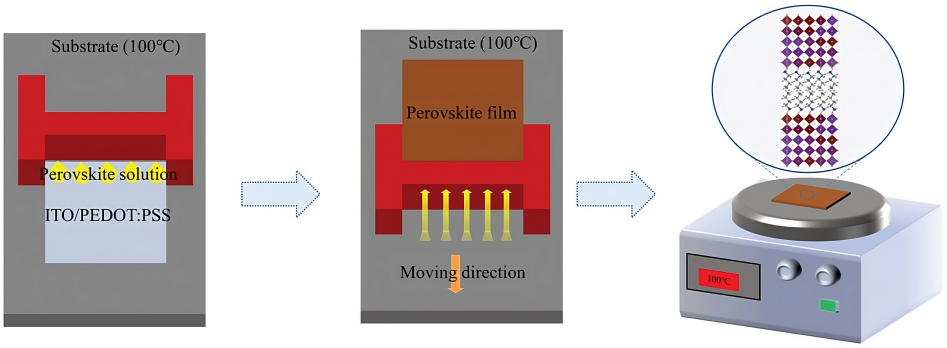

Figure 7: The schematic diagram shows the process of depositing perovskite on a substrate using a blade. The blade coating process is a scalable method that can be used to produce large-area perovskite-based devices. Adapted from [35].

deposited layer, and in this case, it results in a 50 μm thick gold layer on the perovskite material. Au is used as it is more stable on perovskites than other electrodes such as Ag [36].

3.3 Material Physical Properties

3.3.1 Atomic Force Microscopy

Atomic Force Microscopy (AFM) is a powerful imaging technique used to visualize the topography and surface characteristics of materials at the nanoscale. It involves scanning a sharp probe tip across the sample surface while measuring the interaction forces between the tip and the surface. AFM provides high-resolution three-dimensional images, allowing for detailed analysis of surface features [37].

Interpreting an AFM image involves analyzing the surface topography, assessing roughness, examining grain size and morphology and identifying defects and contaminants. The image reveals variations in height, such as steps, peaks, and valleys, providing insights into the sample's surface structure. The density and distribution of surface features indicate surface roughness, while grain size and morphology offer information about the material's crystalline structure. Defects and contaminants can be identified as anomalies on the surface [38]. Correlating AFM data with other characterization techniques further enhances the understanding of the sample. The scanning parameter for the AFM measurement is a square patch with a size 0.2 μm by 0.2 μm. The surface roughness measured is measured within this area.

3.3.2 Spectral Analysis

Spectral analysis, particularly absorbance vs. wavelength measurement, is a fundamental technique used to study the interaction of materials with light across different wavelengths. It provides valuable information about the optical properties and electronic transitions within the material [39]. In the context of Tin Lead perovskite memristors, absorbance spectroscopy can shed light on their light-absorbing capabilities and electronic band structures. Absorbance spectroscopy involves measuring the amount of light absorbed by a material at various wavelengths. A spectrophotometer is commonly used for this purpose. The sample is exposed to a range of wavelengths, and the absorbance of light is recorded [40].

Absorbance (A) is defined as

$$A = -\log_{10}(\frac{I}{I_0})$$

where I is the intensity of light after passing through the sample and I_0 is the intensity before passing

through the sample. Absorbance has no units and ranges from 0 to infinity. An absorbance of 0 means no light is absorbed, an absorbance of 1 means 90% of light is absorbed, 2 means 99% of light is absorbed and so on [41]. Interpreting absorbance spectra involves analyzing the shape, intensity, and position of the absorption peaks. The bandgap energy can be determined from the absorption onset, which corresponds to the minimum energy required to promote an electron from the valence band to the conduction band [42]. By comparing absorbance spectra under different conditions (e.g., temperature, applied voltage), researchers can investigate the influence of external parameters on the optical properties of the memristors. The absorbance is measured for a range of wavelengths covering mainly the visible spectrum. The range of values used here is 300nm to 800nm.

3.4 Probe Station Measurements

3.4.1 Probe Station Setup

The probe station is located within a nitrogen-filled glove box to ensure no contamination with Oxygen or H_2O. The setup consists of two thin Tungsten arms that are angled almost directly downward, both of which can be moved in 3 axes. They are connected to a function generator which is also the measurement device. This component is connected to a computer where the data is collected and sorted. For each device within a sample, a scratch is made to place the negative electrode into. The scratch is made to make sure the bottom electrode can be used as a terminal and this needs to be done as the electrode arms are both placed from the top. This is shown in Figure 8.

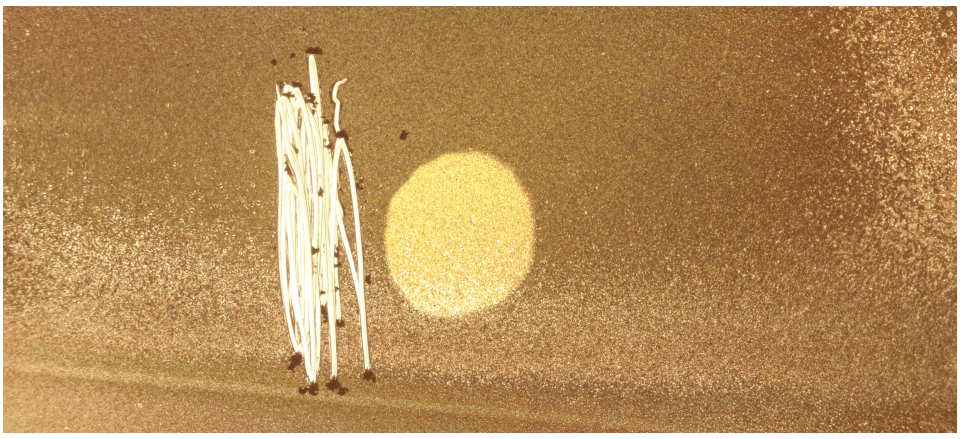

Figure 8: An image of one of the samples. The scratches are made with a scalpel to remove all the layers above the ITO substrate to make it possible to make contact with the bottom electrode. A light is used to illuminate the sample here, though it is kept off during measurements.

3.4.2 IV Measurements

With the probe setup, this measurement is conducted. The probes are placed like Figure 9, where the left and the right probes are the negative and positive electrodes respectively. Programmed through the computer, a bias voltage is passed from the function generator to the sample. The bias voltage for the hysteresis test is set from 0 V to +3 V back to 0 V to -3 V finally back to 0 V to complete the loop. This is conducted over increments of 0.05 V. The results are displayed on a logarithmic graph as this shows a higher level of detail and the values are shown as absolute values so the differences between the positive and negative biases can be seen more easily. The current On/Off ratios are found by dividing the HRS current over the LRS current where at the voltage where the difference between them is its maximum. This will give a measure of the 'height' of the hysteresis.

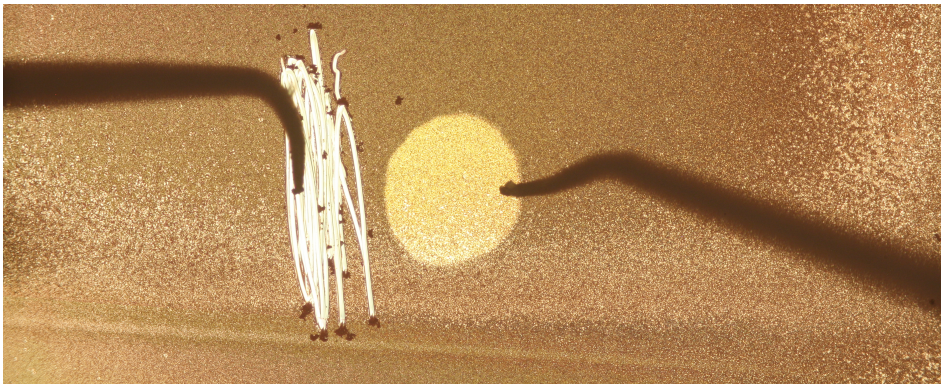

Figure 9: The sample with the probes placed in it. They are placed into position with a system of 3 axis knobs. One of these subsamples can be measured multiple times by moving around the 'needles' in different location within both the brighter circle and the scratch.

3.4.3 Neuromorphic Test

The neuromorphic test is conducted by sending a series of block pulses through the sample and measuring the output. The 'read' voltage is chosen based on the result from the IV measurement and is performed where the hysteresis is the maximum. an up-pulse series is applied where the voltage switches from the read voltage to a chosen 'up pulse value,' increasing its value. This is followed by a series of down pulses where the voltage decreases to another 'down pulse value.' In the specific case of this study, 30 write spikes (+2 V) are applied, followed by 30 erase spikes (-2 V), effectively resetting the system to its initial state. Between each spike, the conductance is allowed to stabilize, and it is subsequently measured using a read pulse (-1.5 V). The pulses are often referred to as the spikes in neural spiking network research [43]. There are other variables as well, pulse width and pulse interval which need to be controlled for a successful result. An example of the settings used is illustrated in Figure 10 alongside what the expected result is one cycle of this test. This value is the setting used for the graph produced in the results section. The settings are unique to each sample and need to be fine-tuned for a successful test.

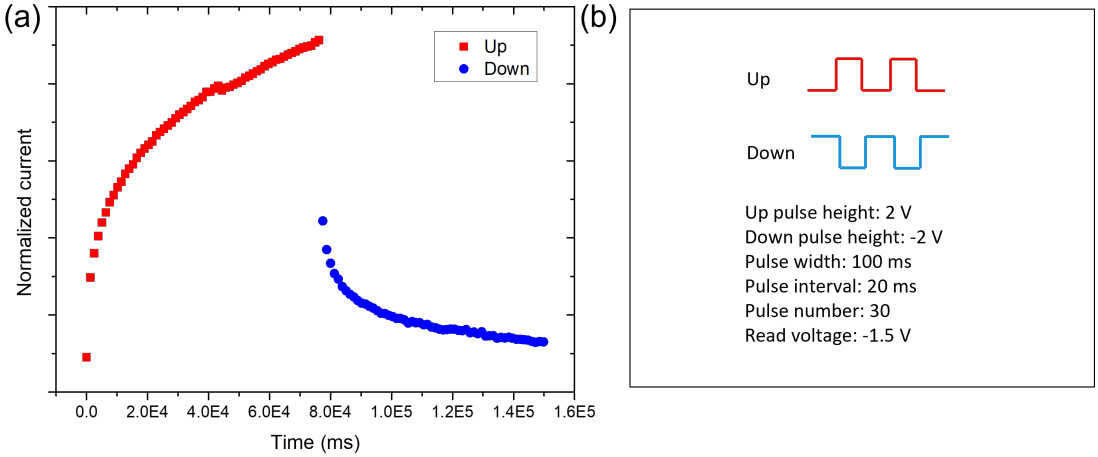

Figure 10: (a) An example of the single cycle expected result of the neuromorphic test. (b) The settings used for the neuromorphic test. It shows the characteristics of the up and down pulses along with other relevant settings.

4 Results

4.1 Atomic Force Microscope

An AFM measurement of a sample of 2D tin lead perovskite is presented in Figure 11 below. There is also a 50 nm scale provided to give a reference of the size of the features within the measurement.

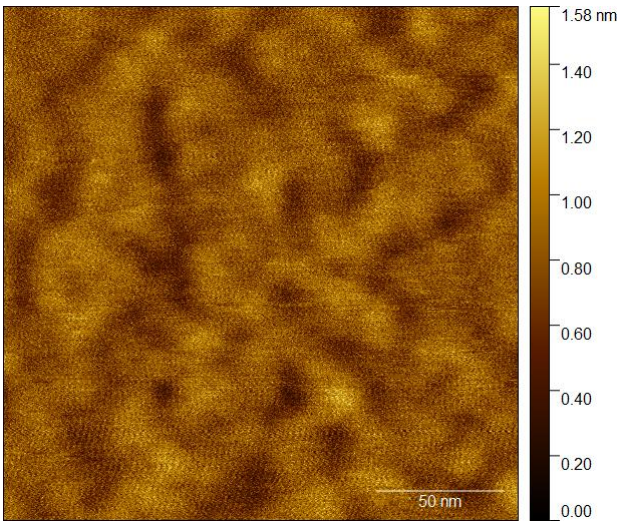

Figure 11: An atomic force microscopy measurement result where the colour bar represents the heights of the features within the sample where black represents the lowest point measured within this result. Heights above this are represented with a brighter colour.

4.2 Spectral Analysis

The UV–Vis absorbance spectral for the 2D tin lead perovskite is shown in Figure 12 where the absorbance value ranges from 0 to 2.

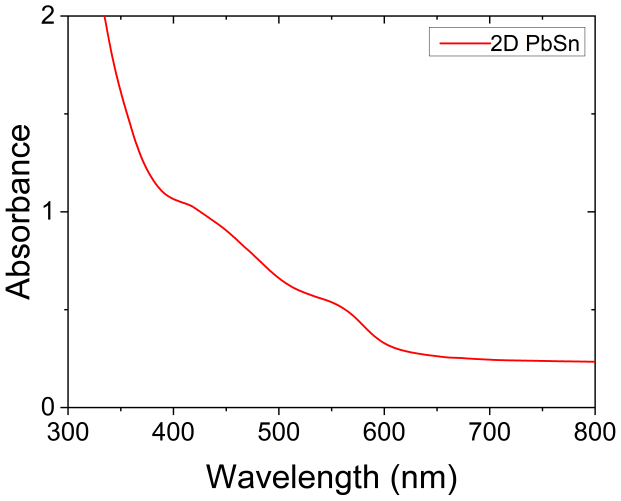

Figure 12: Absorbance spectral data of 2D tin lead perovskite where the height ranges from absorbance values of 0 to 2.

4.3 IV Measurements

4.3.1 Batch 1

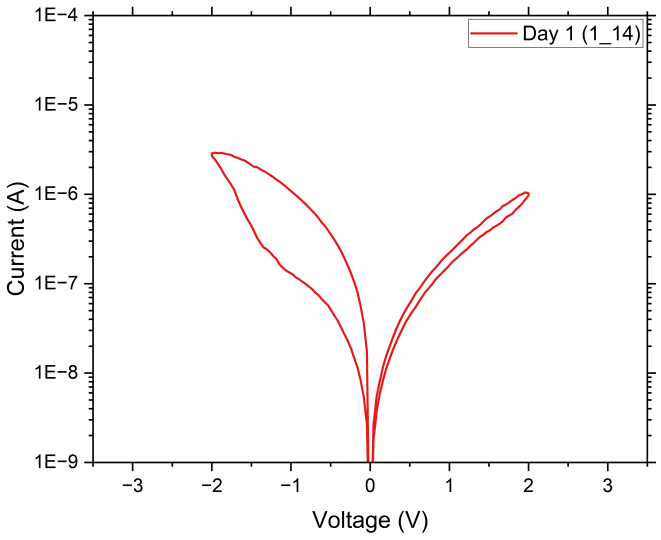

(a) Hysteresis of day 1 (Sample 1_14).

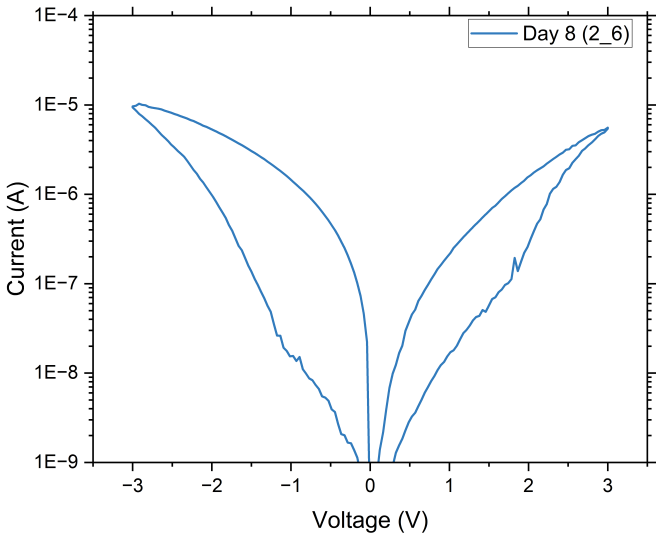

(b) Hysteresis of day 8 (Sample 2_6).

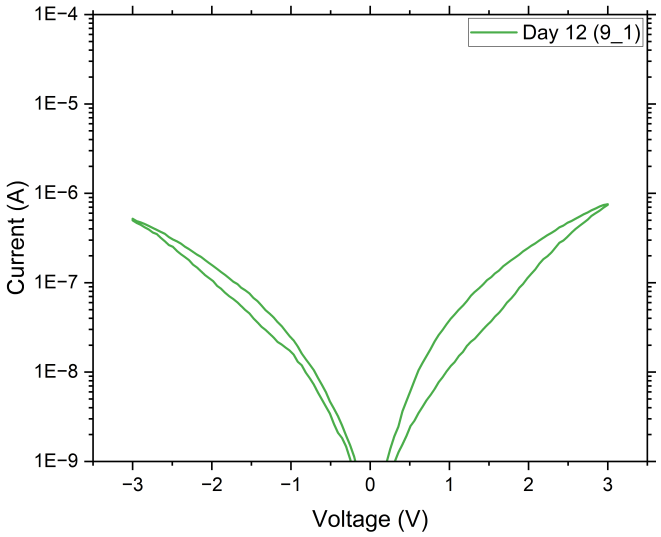

(c) Hysteresis of day 12 (Sample 9_1).

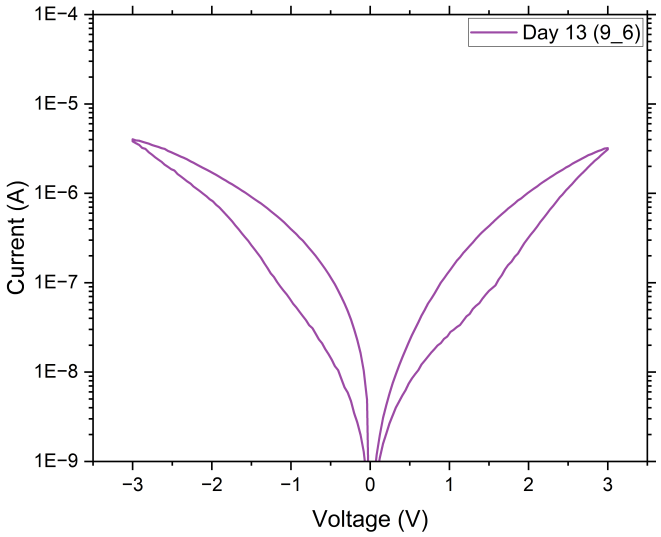

(d) Hysteresis of day 13 (Sample 9_6).

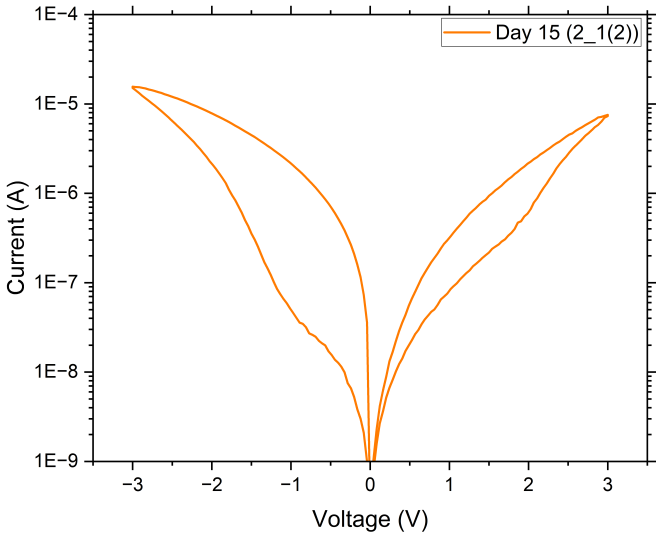

(e) Hysteresis of day 15 (Sample 2_1(2)).

Figure 13: Hysteresis over days from Batch 1.

The maximum current On/Off ratio values for each of the subfigures are respectively 8.63 (Figure 13a), 142 (Figure 13b), 3.41 (Figure 13c), 8.66 (Figure 13d), 348 (Figure 13e). The results in Figure 13 are superimposed together in Figure 14.

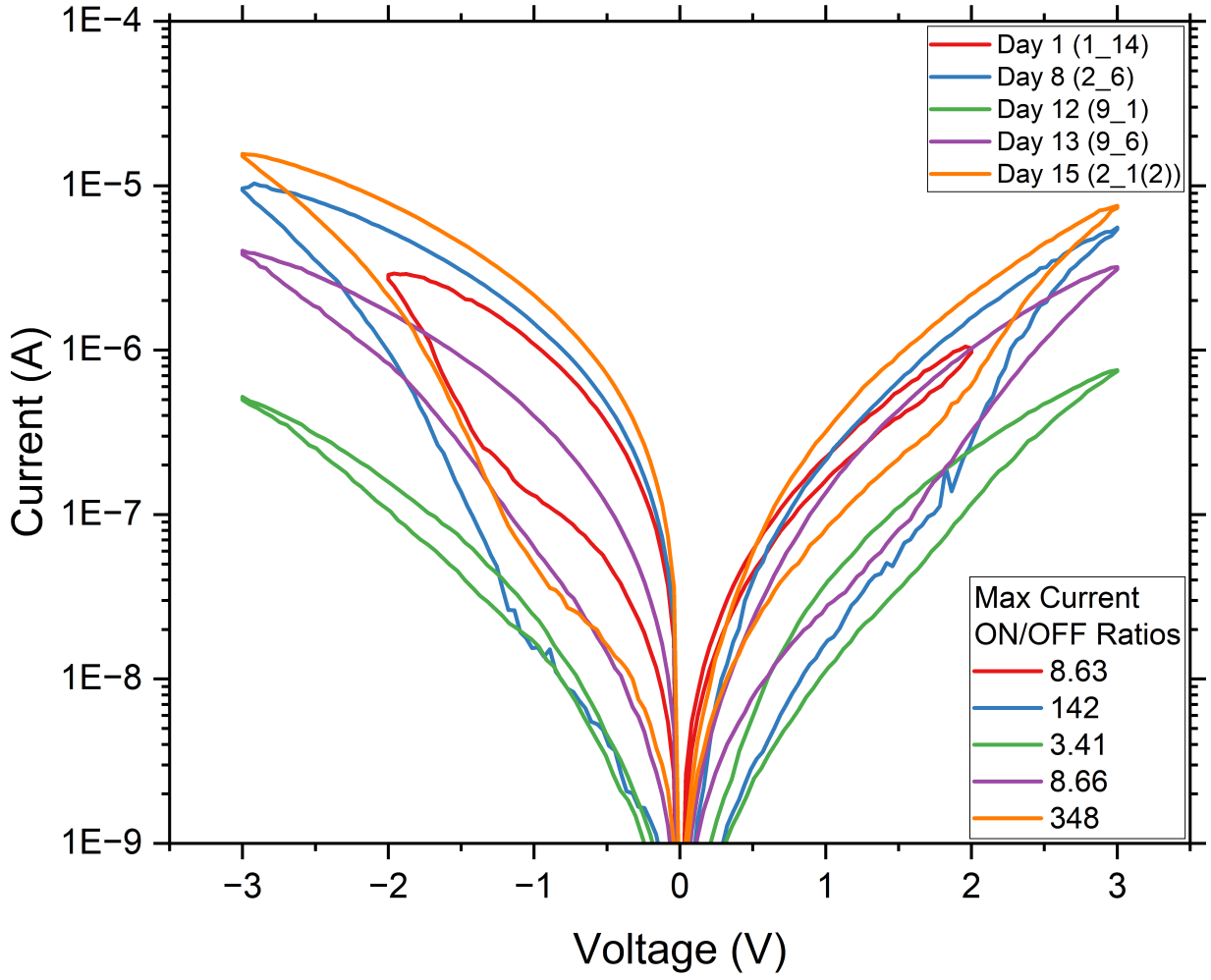

Figure 14: Superimposed hystereses of batch 1 graphs. On the top right corner is the legend giving what colour dictates which day (and sample). The bottom right corner contains the maximum current On/Off ratios for each of the respective samples.

4.3.2 Batch 2

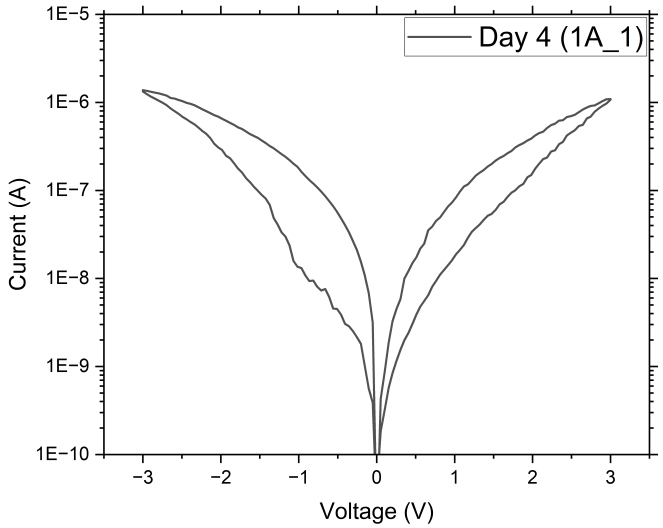

(a) Hysteresis of day 4 (Sample 1A_1).

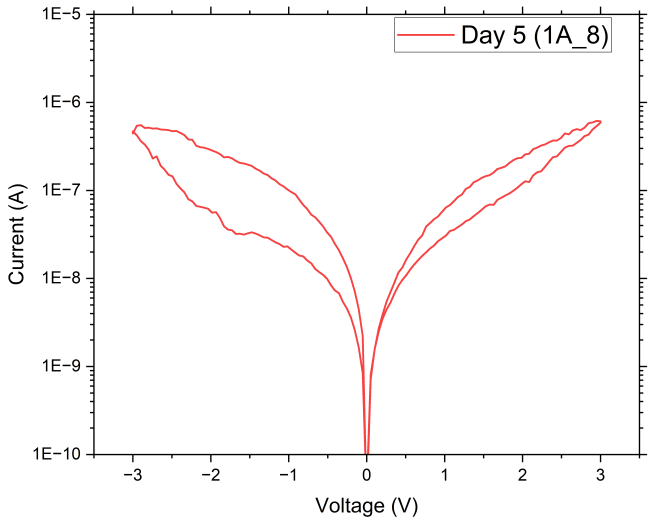

(b) Hysteresis of day 5 (Sample 1A_8).

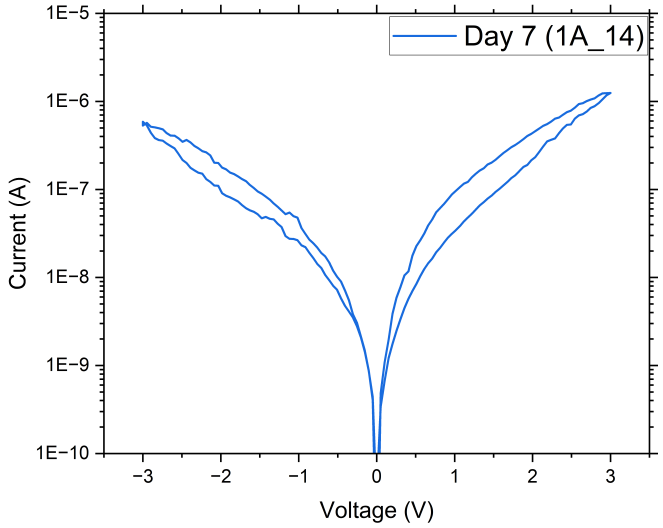

(c) Hysteresis of day 7 (Sample 1A_14).

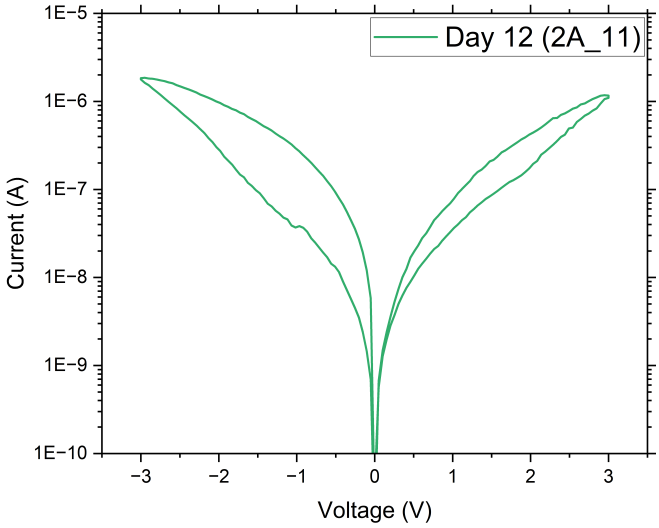

(d) Hysteresis of day 12 (Sample 2A_11).

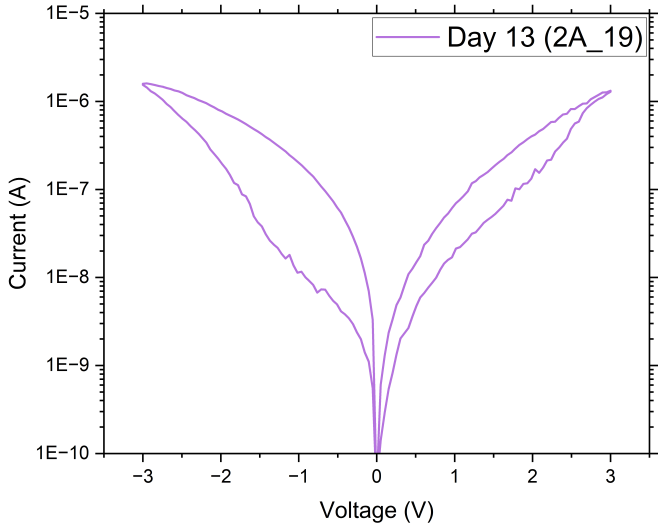

(e) Hysteresis of day 13 (Sample 2A_19).

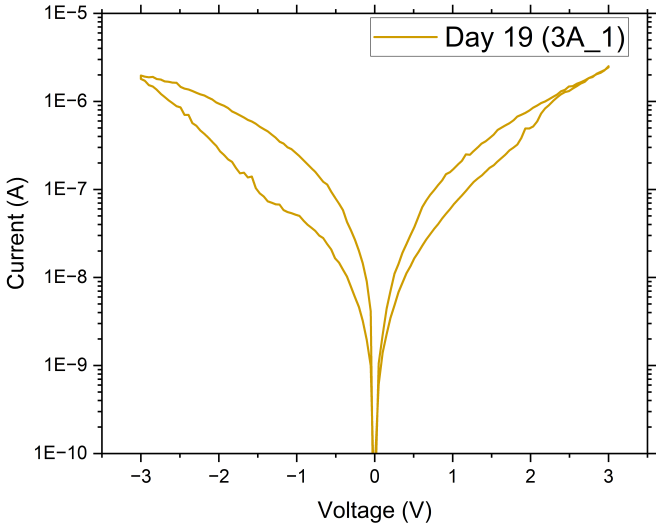

(f) Hysteresis of day 19 (Sample 3A_1).

Figure 15: Hysteresis over days from Batch 2 (Page 1).

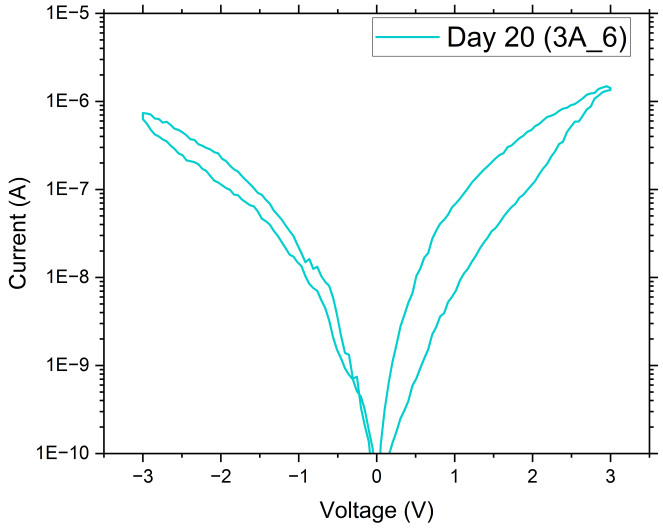

(g) Hysteresis of day 20 (Sample 3A_6).

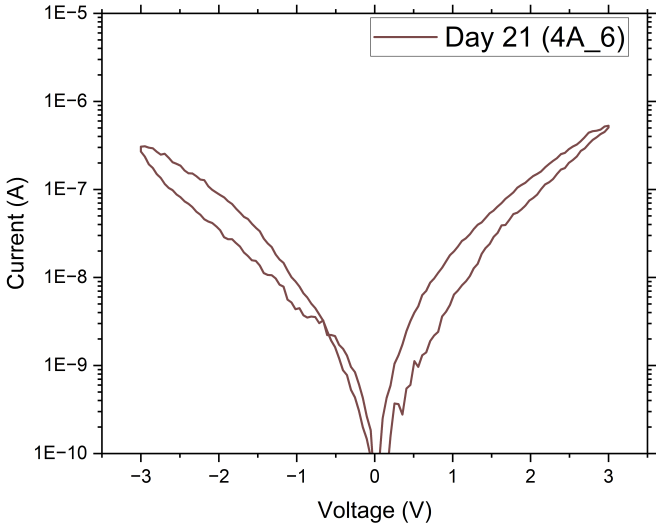

(h) Hysteresis of day 21 (Sample 4A_6).

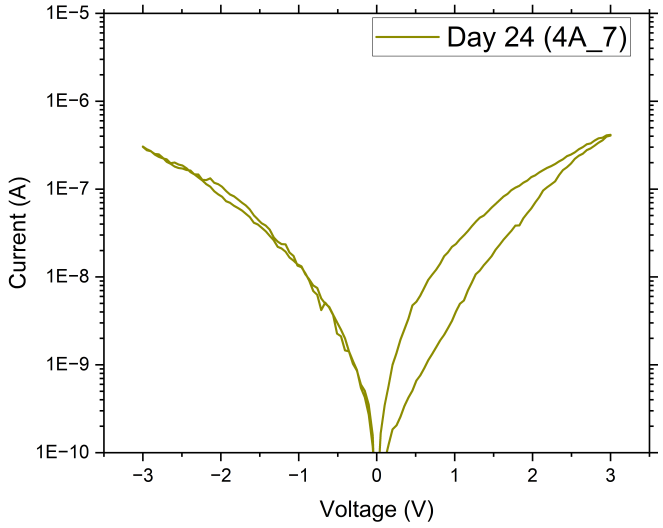

(i) Hysteresis of day 24 (Sample 4A_7).

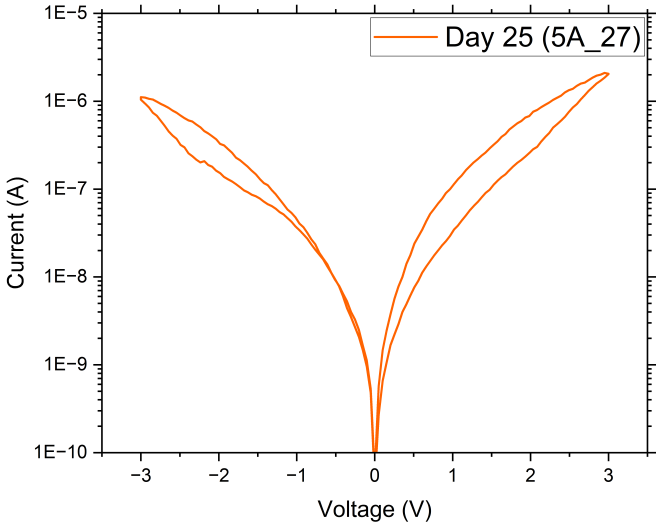

(j) Hysteresis of day 25 (Sample 5A_27).

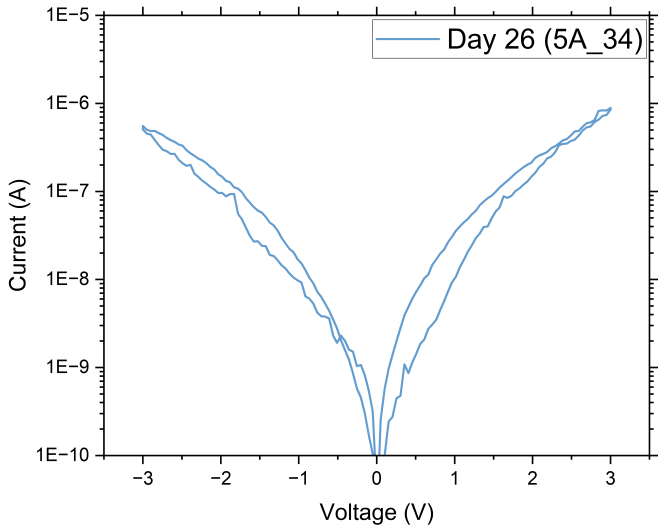

(k) Hysteresis of day 26 (Sample 5A_34).

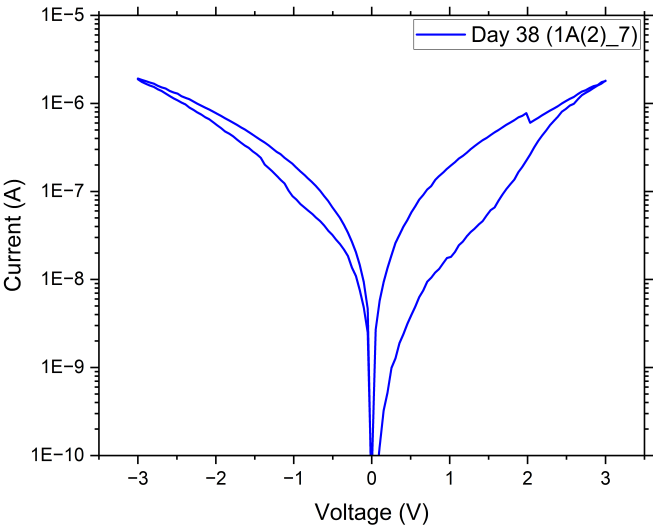

(l) Hysteresis of day 38 (Sample 1A(2)_7).

Figure 15: Hysteresis over days from Batch 2 (Page 2).

The maximum current On/Off ratio values for each of the subfigures are respectively 14.5 (Figure 15a), 6.74 (Figure 15b), 2.85 (Figure 15c), 8.35 (Figure 15d), 19.9 (Figure 15e), 6.23 (Figure 15f), 14.6 (Figure 15g), 6.26 (Figure 15h), 9.34 (Figure 15i), 3.52 (Figure 15j), 5.89 (Figure 15k) and 16.6 (Figure 15l). The results in Figure 15 are superimposed together in Figure 16.

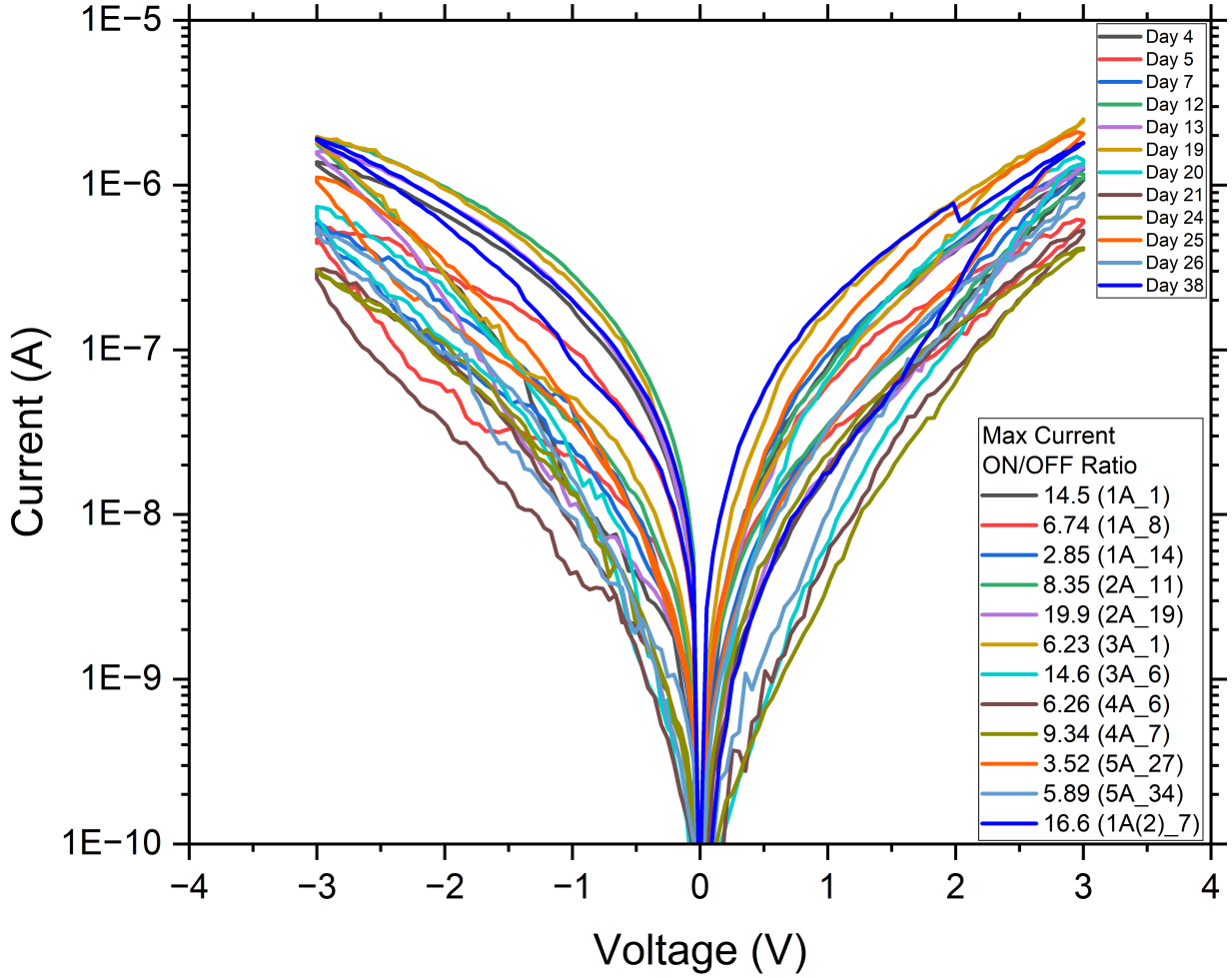

Figure 16: Superimposed hystereses of batch 2 graphs. On the top right corner is the legend giving what colour dictates which day (and sample). The bottom right corner contains the maximum current On/Off ratios for each of the respective samples.

4.4 Neuromorphic Test Measurement

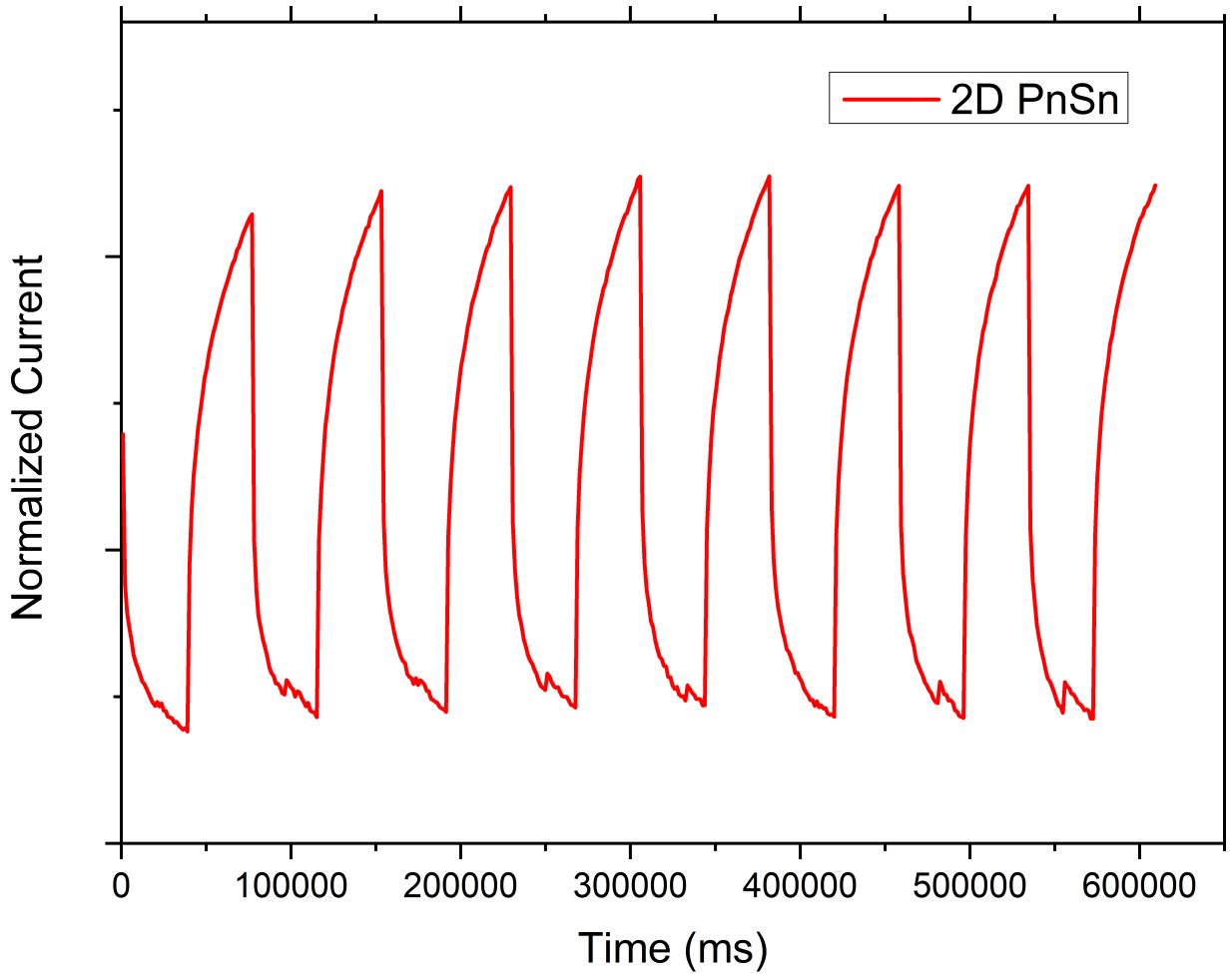

Figure 17: Neuromorphic test with the settings from Figure 10. It is from batch 2, day 5 (Sample 1AN_16). It depicts the test over 8 cycles.

5 Discussion

5.1 AFM and Absorbance Spectral Analysis

From Figure 11, the local surface topography reveals root-mean-square (RMS) roughnesses of our 2D tin lead perovskite is 0.4 nm. The result indicates the obtained perovskite film is very smooth, which is helpful for reproducible and scalable memristors.

From the spectral analysis seen in Figure 12, the absorbance is below 0.32 from 600 nm onwards showing a high absorbance from the mid-visible to UV wavelengths. This means that the perovskite is almost completely transparent to lower visible frequencies like infrared light. The high absorption in the UV-Vis spectrum shows that the bandgap of the active layer has a similar energy to light of this range of wavelengths (600 nm to 300 nm) as given by

$$E = \frac{hc}{\lambda} \tag{2}$$

where E is the energy, h is Planck's constant, c is the speed of light and λ is the wavelength of the light. Since the absorbance falls off at 600 nm, the bandgap of the 2D tin lead perovskites would be around 2.068 eV.

5.2 IV Measurements

5.2.1 Batch 1

Apart from the measurement in the first day (Figure 13a), which has a bias range of ± 2, all the other measurements have a bias of ± 3. As seen in the graphs of the later days, the memristor is able to output proper hystereses until the final measurement of batch 1 on day 15 (Figure 13e). The maximum current On/Off ratios are independent between the samples and as no definitive trend is observed from the first to the last day, no statement can be made about the degradation time of the 2D tin lead perovskite memristors. However, one item to note is that the result from day 8 and day 15 (Figures 13b and 13e) is that they have a similar shape have the two highest values of the current On/Off ratios indicating that within the same sample, the performance will be similar when compared to other samples. This is due to each sample being blade coated separately, possibly having a small amount of variability between them. In the combined graph of Figure 13, most of the figures line up well indicating a low loss of performance between days 1 and 15. This excludes the green graph of day 12 (Figure 13c), which is considered an outlier.

5.2.2 Batch 2

All measurements in this batch have a bias of ± 3. As with batch 1, the measurements during the later days still show reliable memristor performance. However, it looks as the performance becomes more asymmetric between the positive and negative biases, especially in days 20, 21 and 24 (Figures 15g, 15h and 15i respectively). The maximum current On/Off ratios over days in batch 2 is illustrated in Figure 18 shows a slightly upward trend, in contrast to research performed in air [44]. From the combined graph of Figure 15, it can be seen that there is not a high spread of individual graphs showing similar hysteresis performances which indicates the quality of production of each of the samples are similar. More definitively, it shows that the perovskites are still stable and intact by day 38. In fact, it would indicate that 2D tin lead perovskites last more than 38 days at least.

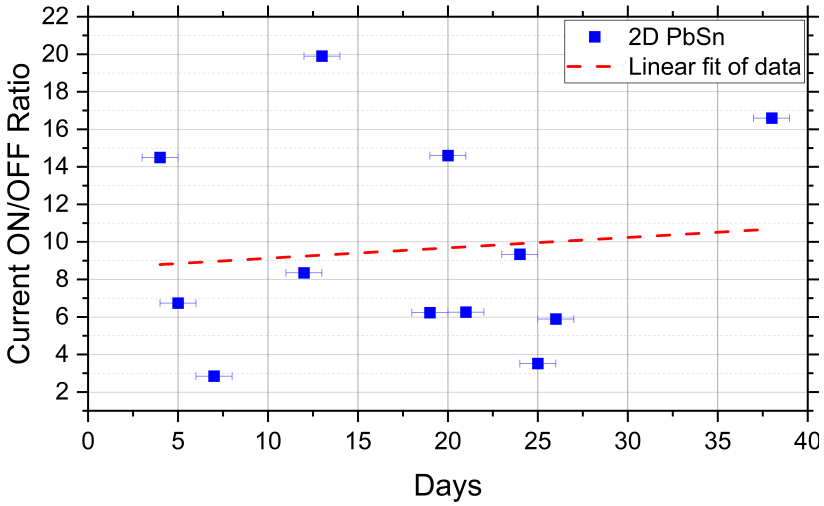

Figure 18: A graphical representation of the maximum measured current On/Off ratios over days. A straight line connects these data points and a dotted line represents a 'best guess' at a linear fit by averaging the values.

5.3 Neuromorphic Test

It can be seen from Figure 17 that the block pulses sent into the memristor show learning behaviour as the numbers of the output pulses increase. It also shows that the memristor is stable enough to withstand at least 8 cycles, run over a period of 10 minutes, of this test before breaking. Furthermore, through this test it can be shown that the effect of the pulse sequences on the current is indeed fully reversible and allows to store an analog variable over long timescales, by applying a series of 60 write and erase spikes over 8 cycles. It can thus be demonstrated that the memristor can be 'programmed' through the changing of the current, enabling the implementation of in-memory operations.

5.4 Limitations of the Investigation

This investigation, while effectively demonstrating many of the key features of perovskite memristors, has some limitations. One significant limitation is the duration of the measurements to show the degradation effects of 2D Tin Lead perovskite memristors. This could not be avoided as the available time for this investigation was fixed and too short. More time would have yielded a more realistic trend as sample recovery outliers would have been smoothed out.

Ideally, the experiments would have been carried out in a controlled environment. However, due to various factors, maintaining a consistent environment was challenging. One factor was the illuminated environment, which was not standardized for all the samples [45]. Additionally, the experiment took place in a vibrationally non-isolated space, which could have caused movements of the probe needles, thereby affecting the results. If the probe moved downward while on top of the thin metal electrode, it could possibly penetrate into lower layers, altering the output current. Furthermore, the presence of other experiments involving evaporation within the same experimental chamber was discovered later, which may have influenced the results.

Moreover, although the glove box used during the experiment had an oxygen concentration of less than 5ppm, prolonged exposure over time could react with the samples, leading to their degradation. However, it is expected that the samples would degrade at a similar rate for this variable.

Lastly, the small sizes of the substrates allowed for a limited number of devices on each sample. Larger substrate sizes would have allowed additional measurements, enabling the averaging of results and segmenting the measurements on a per-sample basis. In other words, one sample could have

been measured throughout the entire study duration and compared with the complete duration measurements of the other samples.

6 Conclusion

In this research project, memristor devices were produced using 2D hybrid tin lead perovskites. The fabrication methods, physical properties, and electrical performance characteristics of these perovskite-based memristor devices were investigated. The environmental sustainability and specific part of the fabrication process, blade coating are some of the highlights of this project.

The results show that the 2D tin lead perovskite films fabricated using blade coating exhibit a smooth surface with a root-mean-square roughness of 0.4 nm, indicating good reproducibility and scalability. The absorbance spectra indicate high absorbance in the mid-visible to UV wavelengths, suggesting a bandgap energy of approximately 2.068 eV. The IV measurements reveal reliable memristor performance over time, with maximum current On/Off ratios varying between samples but no clear degradation trend observed, up to day 38. The maximum current On/Off ratios reached values of up to 348 and 19.9 for batch 1 and batch 2, respectively. The neuromorphic tests demonstrate learning behavior and the stability of the memristors over multiple cycles, indicating their potential for in-memory operations. However, the investigation has limitations in terms of the short measurement duration, environmental inconsistencies and substrate size limitations.

This research on blade-coated 2D tin lead perovskite memristors is important as it contributes to the development of emerging fields in electronics and computing. Memristors, a new class of devices, offer new exciting opportunities for memory storage, neuromorphic computing, and in memory computing architectures. The findings from this study provide insights into the fabrication and characterization of perovskite memristors, displaying their potential for scalable production and neuromorphic applications. With their smooth surface and high absorbance, these memristors can easily be integrated into advanced electronic devices. Potential applications include energy-efficient artificial intelligence, brain-inspired computing, and compact memory systems.

Future research could explore comparative analyses of memristors based on different chemical structures, looking into their performance, stability, and scalability. Fine-tuning the fabrication process, such as optimizing the settings for blade coating and vapor deposition, could improve reproducibility and efficiency of the devices. Moreover, removing lead from the perovskite composition altogether might be a possible option, focusing on alternative materials that offer similar or increased environmental sustainability and reductions in toxicity.

In conclusion, this research on memristors based on perovskite materials highlights their potential for advancements in electronics and computing. With further research, these devices have the capability to revolutionize various applications, paving the way for a more efficient and sustainable future.

7 Acknowledgements

I would like to express my sincere gratitude to Professor Dr. Maria Antonietta Loi, the group leader of the Photophysics and OptoElectronics group, for offering me the opportunity to conduct my bachelor research project in her esteemed research group. It has been an enriching experience to work on the fascinating topic of perovskite memristors within this group.

I am deeply grateful to my daily supervisor, Lijun Chen, for his invaluable support and guidance throughout the project. I would like to thank him for giving me feedback whenever I needed it and always being open to answering questions. More specifically I would also like to thank him for helping me measure the AFM and spectral analysis for the samples.

I would like to thank the technicians of the Photophysics and Opto-electronics group, Arjen Kamp and Teodor Zaharia, for their general technical support. They kept the labs fully functional during my stay and they gave very useful lab tutorials when we needed them.

I am deeply thankful to both my parents and friends back home for their unwavering love and support throughout this research journey. Their encouragement and understanding have been invaluable during the last three months. I would like to offer special thanks to my sister who kept me sane during my entire university journey as well as helping make a figure for this research project.

Lastly, I am filled with heartfelt appreciation for the unwavering support and enduring friendship of the remarkable friends I have had the pleasure of making during my academic journey. Their constant presence and encouragement have been a source of immeasurable strength. I am also deeply grateful to my friends across the globe, whose steadfast support has been an anchor throughout my academic pursuits.

8 References

[1] L. Chua. Memristor-the missing circuit element. *IEEE Transactions on Circuit Theory*, 18(5):507–519, September 1971.

[2] Dmitri B. Strukov, Gregory S. Snider, Duncan R. Stewart, and R. Stanley Williams. The missing memristor found. *Nature*, 453(7191):80–83, May 2008.

[3] Irem Boybat, Manuel Le Gallo, S. R. Nandakumar, Timoleon Moraitis, Thomas Parnell, Tomas Tuma, Bipin Rajendran, Yusuf Leblebici, Abu Sebastian, and Evangelos Eleftheriou. Neuromorphic computing with multi-memristive synapses. *Nature Communications*, 9(1), November 2018.

[4] Doo Seok Jeong, Kyung Min Kim, Sungho Kim, Byung Joon Choi, and Cheol Seong Hwang. Memristors for energy-efficient new computing paradigms. *Advanced Electronic Materials*, 2(9):1600090, Aug 2016.

[5] Hyojung Kim, Min-Ju Choi, Jun Min Suh, Ji Su Han, Sun Gil Kim, Quyet Van Le, Soo Young Kim, and Ho Won Jang. Quasi-2d halide perovskites for resistive switching devices with on/off ratios above 109. *NPG Asia Materials*, 12(1), February 2020.

[6] Xiao Liu, Yanbo Wang, Tianhao Wu, Xin He, Xiangyue Meng, Julien Barbaud, Han Chen, Hiroshi Segawa, Xudong Yang, and Liyuan Han. Efficient and stable tin perovskite solar cells enabled by amorphous-polycrystalline structure. *Nature Communications*, 11(1), May 2020.

[7] Memristors (electronics). `https://www.britannica.com/technology/memristor#/media/1/1430060/126186`. [Online; Accessed 21.06.2023].

[8] Wen Sun, Bin Gao, Miaofang Chi, Qiangfei Xia, J. Joshua Yang, He Qian, and Huaqiang Wu. Understanding memristive switching via in situ characterization and device modeling. *Nature Communications*, 10(1), August 2019.

[9] Leon Chua. Resistance switching memories are memristors. *Applied Physics A*, 102(4):765–783, January 2011.

[10] Xiaoyue Ji, Chun Sing Lai, Guangdong Zhou, Zhekang Dong, Donglian Qi, and Loi Lei Lai. A flexible memristor model with electronic resistive switching memory behavior and its application in spiking neural network. *IEEE Transactions on NanoBioscience*, 22(1):52–62, February 2022.

[11] Fandi Chen, Yingze Zhou, Yanzhe Zhu, Renbo Zhu, Peiyuan Guan, Jiajun Fan, Lu Zhou, Nagarajan Valanoor, Frederic von Wegner, Ed Saribatir, and et al. Recent progress in artificial synaptic devices: Materials, processing and applications. *Journal of Materials Chemistry C*, 9(27):8372–8394, June 2021.

[12] Lingzhi Tang, Yang Huang, Chen Wang, Zhenxuan Zhao, Yiming Yang, Jiming Bian, Huaqiang Wu, Zengxing Zhang, and David Wei Zhang. Halide perovskite memristor with ultra-high-speed and robust flexibility for artificial neuron applications. *Journal of Materials Chemistry C*, 10(39):14695–14702, September 2022.

[13] Quinten A. Akkerman and Liberato Manna. What defines a halide perovskite? *ACS Energy Letters*, 5(2):604–610, January 2020.

[14] History of perovskite solar cells. `www.g2voptics.com/history-of-perovskite-solar-cells`. [Online; Accessed 21.06.2023].

[15] Guo Jia, Ze-Jiao Shi, Ying-Dong Xia, Qi Wei, Yong-Hua Chen, Gui-Chuan Xing, and Wei Huang. Super air stable quasi-2d organic-inorganic hybrid perovskites for visible light-emitting diodes. *Optics Express*, 26(2), Decemeber 2017.

[16] Lingling Mao, Constantinos C. Stoumpos, and Mercouri G. Kanatzidis. Two-dimensional hybrid halide perovskites: Principles and promises. *Journal of the American Chemical Society*, 141(3):1171–1190, November 2018.

[17] Bikash Kumar Shaw, Ashlea R. Hughes, Maxime Ducamp, Stephen Moss, Anup Debnath, Adam F. Sapnik, Michael F. Thorne, Lauren N. McHugh, Andrea Pugliese, Dean S. Keeble, and et al. Melting of hybrid organic–inorganic perovskites. *Nature Chemistry*, 13(8):778–785, May 2021.

[18] Rohit Abraham John, Nimesh Shah, Sujaya Kumar Vishwanath, Si En Ng, Benny Febriansyah, Metikoti Jagadeeswararao, Chip-Hong Chang, Arindam Basu, and Nripan Mathews. Halide perovskite memristors as flexible and reconfigurable physical unclonable functions. *Nature Communications*, 12(1), June 2021.

[19] Manuel Kober-Czerny, Silvia Genaro Motti, Philippe Holzhey, Bernard Wenger, Jongchul Lim, Laura Maria Herz, and Henry James Snaith. Excellent long-range charge-carrier mobility in 2d perovskites. *Advanced Functional Materials*, (36):2203064, June 2022.

[20] David O'Connor and Deyi Hou. Manage the environmental risks of perovskites. *One Earth*, 4(11):1534–1537, Nov 2021.

[21] Mahdi Malekshahi Byranvand, Weiwei Zuo, Roghayeh Imani, Meysam Pazoki, and Michael Saliba. Tin-based halide perovskite materials: Properties and applications. *Chemical Science*, 13(23):6766–6781, May 2022.

[22] Kimberley J. Savill, Aleksander M. Ulatowski, and Laura M. Herz. Optoelectronic properties of tin–lead halide perovskites. *ACS Energy Letters*, 6(7):2413–2426, June 2021.

[23] Spyros Stathopoulos, Loukas Michalas, Ali Khiat, Alexantrou Serb, and Themis Prodromakis. An electrical characterisation methodology for benchmarking memristive device technologies. *Scientific Reports*, 9(1), December 2019.

[24] Lingzhi Tang, Yang Huang, Chen Wang, Zhenxuan Zhao, Yiming Yang, Jiming Bian, Huaqiang Wu, Zengxing Zhang, and David Wei Zhang. Halide perovskite memristor with ultra-high-speed and robust flexibility for artificial neuron applications. *Journal of Materials Chemistry C*, 10(39):14695–14702, September 2022.

[25] Feng Wang, Sai Bai, Wolfgang Tress, Anders Hagfeldt, and Feng Gao. Defects engineering for high-performance perovskite solar cells. *npj Flexible Electronics*, 2(1), July 2018.

[26] Von neumann machine. `https://www.britannica.com/technology/von-Neumann-machine`. [Online; Accessed 21.06.2023].

[27] C. Mead. Neuromorphic electronic systems. *Proceedings of the IEEE*, 78(10):1629–1636, October 1990.

[28] I I Arikpo, F U Ogban, and I E Eteng. Von neumann architecture and modern computers. *Global Journal of Mathematical Sciences*, 6(2), July 2008.

[29] Sergei Petrenko. Limitations of von neumann architecture. *Big Data Technologies for Monitoring of Computer Security: A Case Study of the Russian Federation*, page 115–173, May 2018.

[30] J. Grollier, D. Querlioz, K. Y. Camsari, K. Everschor-Sitte, S. Fukami, and M. D. Stiles. Neuromorphic spintronics. *Nature Electronics*, 3(7):360–370, March 2020.

[31] Suhas Kumar, Xinxin Wang, John Paul Strachan, Yuchao Yang, and Wei D. Lu. Dynamical memristors for higher-complexity neuromorphic computing. *Nature Reviews Materials*, 7(7):575–591, July 2022.

[32] Wen-Fa Wu and Bi-Shiou Chiou. Effect of annealing on electrical and optical properties of rf magnetron sputtered indium tin oxide films. *Applied Surface Science*, 68(4):497–504, August 1993.

[33] 1,5-dan. `http://www.chemspider.com/Chemical-Structure.15851.html`. [Online; Accessed 25.06.2023].

[34] O. Yu. Posudievsky, N.V. Konoshchuk, A.G. Shkavro, V.G. Koshechko, and V.D. Pokhodenko. Structure and electronic properties of poly(3,4-ethylenedioxythiophene) poly(styrene sulfonate) prepared under ultrasonic irradiation. *Synthetic Metals*, 195:335–339, July 2014.

[35] Lijun Chen, Jun Xi, Eelco Kinsa Tekelenburg, Karolina Tran, Giuseppe Portale, Christoph J Brabec, and Maria Antonietta Loi. Quasi-2d lead–tin perovskite memory devices fabricated by blade coating. *Small Methods*, June 2023.

[36] Fangfang Wang, Yezhou Cao, Cheng Chen, Qing Chen, Xiao Wu, Xinguo Li, Tianshi Qin, and Wei Huang. Materials toward the upscaling of perovskite solar cells: Progress, challenges, and strategies. *Advanced Functional Materials*, 28(52):1803753, November 2018.

[37] M.K. Khan, Q.Y. Wang, and M.E. Fitzpatrick. Atomic force microscopy (afm) for materials characterization. *Materials Characterization Using Nondestructive Evaluation (NDE) Methods*, page 1–16, April 2016.

[38] Greg Haugstad. *Atomic Force Microscopy: Understanding basic modes and advanced applications*. Wiley, 2012.

[39] Light absorption and photoluminescence (PL) spectroscopy, August 2022. [Online; Accessed 25.06.2023].

[40] Timothy J. Peshek, Justin S. Fada, and Ina T. Martin. Degradation processes in photovoltaic cells. *Durability and Reliability of Polymers and Other Materials in Photovoltaic Modules*, page 97–118, July 2019.

[41] Allan Robinson. How to calculate the percent transmittance. `https://sciencing.com/calculate-percent-transmittance-7599639.html`, March 2018. [Online; Accessed 26.06.2023].

[42] Patrycja Makuła, Michał Pacia, and Wojciech Macyk. How to correctly determine the band gap energy of modified semiconductor photocatalysts based on uv–vis spectra. *The Journal of Physical Chemistry Letters*, 9(23):6814–6817, December 2018.

[43] P. Robin, T. Emmerich, A. Ismail, A. Niguès, Y. You, G.-H. Nam, A. Keerthi, A. Siria, A. K. Geim, B. Radha, and et al. Long-term memory and synapse-like dynamics in two-dimensional nanofluidic channels. *Science*, 379(6628):161–167, January 2023.

[44] Vincent J.-Y. Lim, Aleksander M. Ulatowski, Christina Kamaraki, Matthew T. Klug, Laura Miranda Perez, Michael B. Johnston, and Laura M. Herz. Air-degradation mechanisms in mixed lead-tin halide perovskites for solar cells. *Advanced Energy Materials*, page 2200847, May 2022.

[45] Laura E. Mundt, Jinhui Tong, Axel F. Palmstrom, Sean P. Dunfield, Kai Zhu, Joseph J. Berry, Laura T. Schelhas, and Erin L. Ratcliff. Surface-activated corrosion in tin–lead halide perovskite solar cells. *ACS Energy Letters*, 5(11):3344–3351, September 2020.